A Foreground-background Parallel Compression with Residual Encoding for Surveillance Video

Lirong Wu, *Student Member, IEEE*, Kejie Huang, *Senior Member, IEEE*, Haibin Shen, and Lianli Gao

Abstract—The data storage has been one of the bottlenecks in surveillance systems. The conventional video compression algorithms such as H.264 and H.265 do not fully utilize the low information density characteristic of the surveillance video. In this paper, we propose a video compression method that extracts and compresses the foreground and background of the video separately. The compression ratio is greatly improved by sharing background information among multiple adjacent frames through an adaptive background updating and interpolation module. Besides, we present two different schemes to compress the foreground and compare their performance in the ablation study to show the importance of temporal information for video compression. In the decoding end, a coarse-to-fine two-stage module is applied to achieve the composition of the foreground and background and the enhancements of frame quality. Furthermore, an adaptive sampling method for surveillance cameras is proposed, and we have shown its effects through software simulation. The experimental results show that our proposed method requires 69.5% less bpp (bits per pixel) than the conventional algorithm H.265 to achieve the same PSNR (36 dB) on the HECV dataset.

Index Terms—Surveillance video, background modeling, deep neural network, video coding.

I. INTRODUCTION

NOWADAYS, video content contributes more than 90% of network traffic, and this percentage is expected to further increase in the future [1]. The current mainstream video compression algorithms are H.264 [2] and H.265 [3]. Recently, many DNN-based video compression algorithms are under focused development to achieve higher compression ratio with less distortion than conventional algorithms [4]–[6]. Among various videos, surveillance video is expanding exponentially due to the importance of real-time analytics, and the increased popularity of Machine Learning (ML) and Artificial Intelligence (AI). With more data being created by video content and analytics, the compression and storage of surveillance videos have become an increasingly hot research topic. However, both non-DNN and DNN based algorithms still have room to improve in the field of surveillance video compression, because they do not fully utilize the low information density characteristic in the video, such as unmanned streets and static backgrounds. Besides, there is strong temporal relevance between adjacent frames in the surveillance video and each frame can be divided into two parts: background

Lirong Wu, Kejie Huang, and Haibin Shen are with the Department of Information Science & Electronic Engineering, Zhejiang University, Hangzhou 310027, China, e-mail: {wulirong, huangkejie, shen_hb}@zju.edu.cn.

Lianli Gao is with the School of Computer Science and Engineering, University of Electronic Science and Technology of China, Chengdu, 611731, China, e-mail: lianli.gao@uestc.edu.cn

and foreground. The violent fluctuations of video contents often occur in the foreground regions, while the contents of the background are constant and static. Therefore, it is not necessary to attach equal importance to the background as to the foreground during compression, which may inevitably lead to redundancy.

In this paper, we propose a novel method to greatly reduce the compression ratio of the surveillance video while keeping similar video quality. To achieve this, the foreground and background are extracted and compressed separately from the surveillance video and the compression bitstreams are indexed to facilitate retrieval. To compress the foreground, we propose a motion-based method with residual encoding, which estimates, compensates and predicts the motion of the foreground objects based on the optical flow information and then encodes the residuals. In addition, the ideas of the template updating and background interpolation are applied to background compression. We design an adaptive background template updating algorithm to pick the backgrounds of keyframes as templates. Then we perform residual encoding on those background templates and compute corresponding backgrounds between adjacent templates through interpolation. It can automatically make a trade-off between distortion and compression ratio, and overcome the problem that it is difficult to find a suitable fixed interval for the background template updating.

As for the decompression of the video, we propose a novel coarse-to-fine, two-stage module. The first stage is a composite module that composites the foreground and background into a complete frame. The second stage is a reconstruction network (Rec-Net) that optimizes the composite frames by eliminating boundaries, blurring, and other distortion. The experimental results show that our model outperforms the widely used algorithms, such as H.264 and H.265 when measured by the Multiscale Structural Similarity Index (MS-SSIM) [7] and Peak Signal to Noise Ratio (PSNR). Our contributions are listed in the following:

- We propose a DNN-based method to compress the foreground and background of the surveillance video in two different schemes separately.
- We present an adaptive background updating and interpolation algorithm to replace tedious handcrafted settings.
- We perform compression on the foreground of video via a motion-based method with residual encoding and then demonstrate the importance of temporal information to video compression in the ablation experiment.
- We achieve video composite and reconstruction through a coarse-to-fine, two-stage decoding module.
- We contribute a novel idea to perform adaptive sampling

for surveillance cameras and show its effect through software simulation.

The rest of the paper is organized as follows: In Section II, some common video compression algorithms and techniques are briefly reviewed. Section III describes the entire architecture of our model and the details of each part. In Section IV and Section V, we present our implementation details and experimental results, respectively. Section VI analyzes and summarizes our results, and Section VII draws the conclusion.

II. RELATED WORK

A. Conventional Video Compression

H.264 and H.265 have been widely used in video compression in recent decades. These algorithms have a similar architecture, which contains three types of frames: I-frames, P-frames, and B-frames. Recently, many algorithms specially designed for surveillance videos are under focused development on this basis. For example, Zhang et al. propose a Background-Modeling Adaptive Prediction method BMAP [8]. Its basic idea is to adopt different prediction methods based on the classification results of blocks. Unlike this, the method BDC directly codes the difference between the input frame and the reconstructed background modeled from the original video [9]. In addition, Chen et al. propose a Block-Composed Background Reference method BCBR to generate the background reference gradually by block updating instead of picture updating [10]. The proposed background reference is implemented into High Efficiency Video Coding (HEVC), and the experimental results demonstrate a significant improvement in coding efficiency. Besides, a background modeling and referencing scheme for moving cameras-captured surveillance video coding in HEVC is proposed by [11]. Unlike these, Ma et al. build a library of foreground (vehicles) to search for similar vehicles and use the retrieved results to help encode [12]. However, library-based methods are often not practical because it is difficult to build multiple libraries for all objects that may appear in the surveillance video. The above methods all follow the conventional architecture, which includes components such as motion estimation, motion compensation, etc.

B. DNN-based Video Compression

In recent years, DNN-based video compression is under intensive development. The majority of DNN-based schemes improve compression performance by optimizing and improving the certain component of the conventional video compression architecture. For example, Lu et al. propose an end-to-end Deep Video Compression framework DVC [5]. They replace the components such as motion estimation and motion compensation with DNNs to improve performance. What's more, the DNN-based optical flow map is also used as an effective motion estimation method in the work of [5], [13]. Besides, Wu et al. use an RNN-based Key-Frame Interpolation method KFI to generate non-key frames by keyframe interpolation and finally synthesize the complete video [6].

Since Generative Adversarial Network (GAN) is proposed [14], the idea of adversarial training has been applied to the field of compression [15]–[17]. For example, [4] applies GAN to frame prediction and interpolation to achieve video compression. However, long-term prediction and interpolation can cause severe distortion, so this interpolation method heavily relies on handcrafted settings, such as the selection of keyframes. Furthermore, Yang et al. propose a Multi-Frame Quality Enhancement algorithm MFQE that uses high-quality frames to enhance the quality of low-quality frames based on the fluctuations of compressed video frame quality [18]. In addition, many video compression methods have been proposed for intra-prediction [19], [20], inter-prediction [16], [21], post-processing [22], and mode decision [23]. However, to the best of our knowledge, there is currently no efficient DNN-based method for surveillance video compression.

C. Video Background Modeling

The background modeling can separate the foreground and background of the frame and generate an image containing only the background contents. This background image can be used as a long-term reference for encoding subsequent frames. A simple method is to treat the long-term average of several frames as the background image. However, this method requires a large number of frames and often fails when the foreground objects remain stationary.

To solve the above problems, there are two types of background modeling methods: non-parameterized [24]–[26] and parameterized [27]–[30]. For example, Elgammal et al. propose a nonparametric method to estimate the probability density of a given pixel using kernel density estimation based on historical data [24]. Non-parameterized methods often perform well in highly dynamic scenes, but they are not efficient enough due to the high computational complexity. In real-time applications such as object tracking and video compression, many parameterized methods are applied. For example, the Gaussian Mixture Model (GMM) is proposed, which models each pixel of a scene independently through a mixture of four Gaussian distributions [27]. However, these methods often require handcrafted settings of specific parameters based on the application scenario. For this reason, many improved versions of these methods have been proposed, such as the improved GMM with adaptive parameters used in this paper [30]. The background modeling module in our architecture is replaceable, which means we can replace it with better methods for higher performance and efficiency in the future, but this is beyond the scope of this paper.

III. MODEL ARCHITECTURE

Fig. 1 provides a high-level overview of our video compression architecture. The red (S1-S2) and green (S3-S7) modules are responsible for the compression of the background and foreground, respectively. The blue (S8) modules represent a coarse-to-fine two-stage module, which achieves the composition of foreground and background and the enhancements of frame quality. It should be noted that the yellow lines (imaginary lines) in the Fig. 1 represent the decoding process, which reconstructs video frames based on the received bitstreams. Let $\mathbb{V} = \{x_1, x_2, \ldots, x_{t-1}, x_t, \ldots\}$ represents a video sequence,
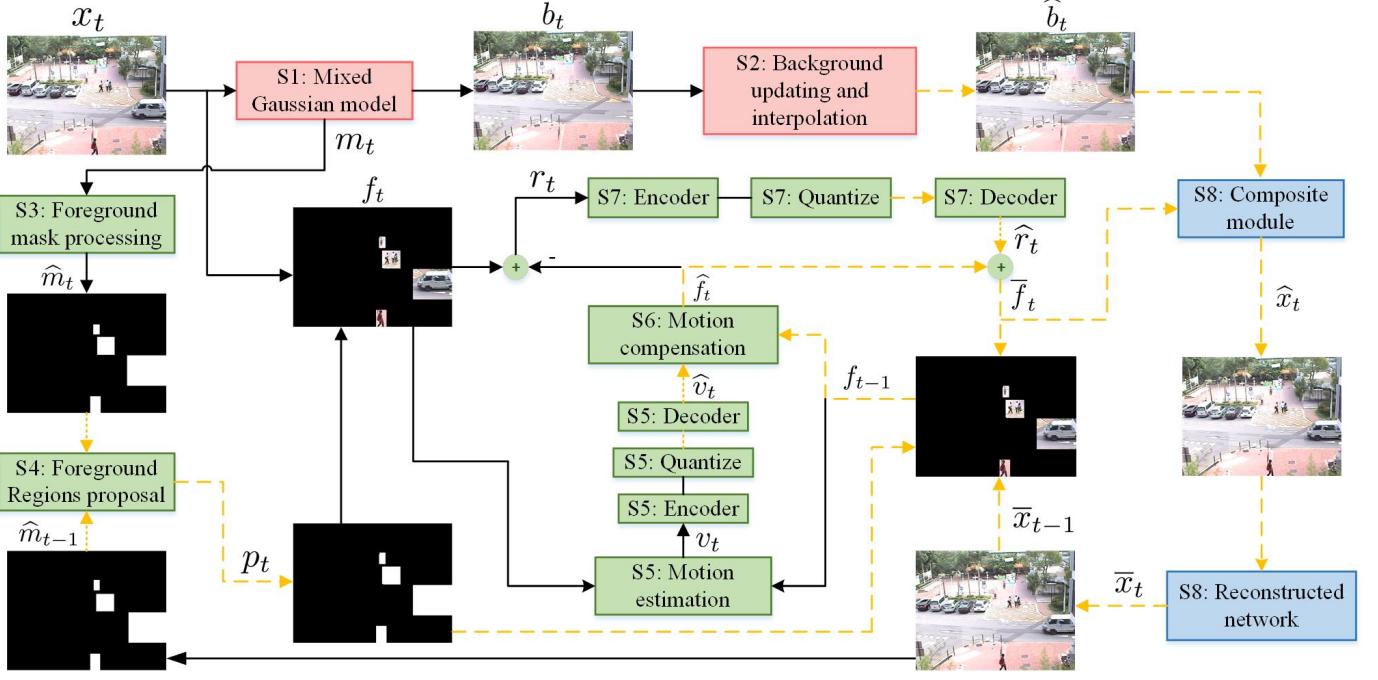
Fig. 1. Illustration of our video compression architecture. The red (S1-S2) and green (S3-S7)modules are responsible for the compression of the background and foreground, respectively. The blue (S8) module represents a coarse-to-fine two-stage module, which achieves the composition and enhancements of frames. It should be noted that the yellow lines (imaginary lines) in the figure represent the decoding process, which reconstructs video frames based on the received bitstreams.

where x_t represents the frame at time t. The overall procedure is described in section. III-A, and some important components will be detailed in the remaining sections.

A. Overall Procedure

Step 1 Foreground-background separation. Following the method proposed in [30], we use an adaptive Gaussian mixture model to separate frame x_t into background b_t and foreground mask m_t sequentially.

Step 2 Adaptive background updating and interpolation. Since the context of the background is generally constant, we can improve the compression ratio by sharing the background information among multiple adjacent frames. The updating and interpolation of the background are controlled by an adaptive background updating and interpolation module, where the current background b_t is the input of the reconstructed background $\widehat{b}_t$. This step will be described in detail in Sec. III-B.

Step 3 Foreground masks processing. We perform the morphological process on the foreground mask m_t to eliminate noise, and then get the desired regular foreground mask $\widehat{m}_t$ through simple bounding rectangle search [31]. This step will be described in detail in Sec. III-C.

Step 4 Foreground regions proposal. We merge the foreground regions of $\widehat{m}_{t-1}$ and $\widehat{m}_t$ to get a new mask p_t. Under the guidance of the mask p_t, we can get the foreground f_{t-1} and f_t from the original frame $\overline{x}_{t-1}$ and x_t, respectively.

Step 5 Motion estimation. Instead of conventional block-based motion estimation, we use the optical flow for motion estimation. Specifically, we use the model proposed in [32] to estimate the optical flow, that is, the motion information v_t.

To further improve the compression ratio, we encode, quantize and decode v_t to obtain $\widehat{v}_t$. The specific network structure of the information codec (encoder and decoder) is provided in the appendix. If the size of the input v_t is $H \times W \times 3$, then the size of encoding result is $\frac{H}{8} \times \frac{W}{8} \times C$. Setting C to different values produces different compression ratios, which is a trade-off between the compression ratio and the distortion.

Step 6 Motion compensation. A motion compensation module is designed to predict the foreground $\widehat{f}_t$ of the next frame based on optical flow $\widehat{v}_t$ and previous foreground f_{t-1}. This step will be described in detail in Sec. III-D.

Step 7 Residual coding. The residual r_t between the original foreground f_t and the predicted foreground $\widehat{f}_t$ is obtained as $r_t = f_t$ - $\widehat{f}_t$. Similarly, we use the same information codec as in Step 5 to encode, quantize, and decode r_t to obtain $\widehat{r}_t$. Then we get the reconstructed foreground $\overline{f}_t = \widehat{r}_t + \widehat{f}_t$

Step 8 Two-stage decoding module. The composite module and Rec-Net make up a coarse-to-fine two-stage module. The composite module combines $\overline{f}_t$ with the background $\widehat{b}_t$ to generate a composite frame $\widehat{x}_t$. The Rec-Net enhances the quality of the composite frame $\widehat{x}_t$ by eliminating the artifacts, blurring and boundaries and produces a visually more realistic frame $\overline{x}_t$. This step will be described in detail in Sec. III-E.

B. Adaptive background updating and interpolation

Although the background of surveillance video is visually static, it actually has fluctuations in the brightness and color caused by the change of the lighting, weather, and time [18]. Therefore, we can select an initial background template, then update the template according to the changing intensity of

the background, and finally computing the remaining backgrounds by frame interpolation between adjacent templates. The background template can be updated at equal interval l, which means b_t, b_{t+l}, b_{t+2l}, … are selected as the background templates. However, it is not easy to determine a suitable fixed interval l. If the l is too large, the template may not respond to a fast and intense background change. If the l is too small, the compression ratio will be reduced, which is contrary to our original intention. To address it, an adaptive background template updating algorithm is proposed in this paper.

We compare the background b_t extracted from each frame with the previous background template B_{t-m}. For example, we can calculate the MS-SSIM of b_t and B_{t-m}. As shown in Fig. 2, if the value is smaller than the threshold γ, we perform the residual coding on the background b_t as in Step 7 of III-A to get the current background template B_t. After that, we can get the rest of the backgrounds $\widehat{b}_{t-m+1}, ..., \widehat{b}_{t-1}$ between adjacent templates B_{t-m} and B_t through linear interpolation, formulated as

$$\widehat{\mathbf{b}}_{t-j}(i) = \mathbf{B}_{t-m}(i) + (\mathbf{B}_t(i) - \mathbf{B}_{t-m}(i)) \times \frac{m-j}{m} \quad (1)$$

where $\widehat{\mathbf{b}}_{t-j}$ denotes the reconstructed background at time $b-j$ and $\mathbf{B}_t$ denotes the background template at time t. Besides, $j \in (\{0, 1, ..., m\})$, i enumerates all positions in $\widehat{\mathbf{b}}$ and $\mathbf{B}$, and m is the interval of two adjacent templates $\mathbf{B}_{t-m}$ and $\mathbf{B}_t$. In addition, we also use a more complex CNN-based video frame interpolation method for background interpolation, and present a trade-off between the two through experiments.
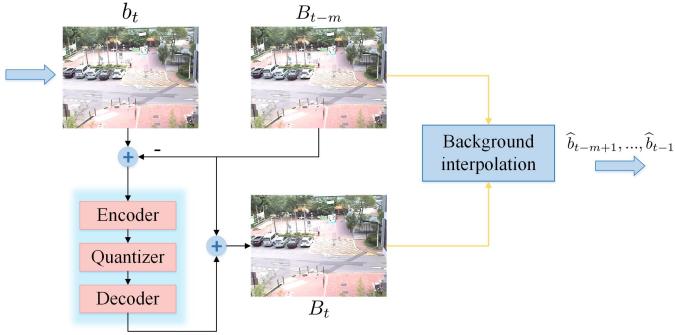

Fig. 2. Illustration of the adaptive background updating and interpolation.

C. Foreground Masks Processing

As shown in Fig. 3, the foreground mask m_t obtained by the Gaussian mixture model [30] contains a lot of noise and cannot be directly used to guide foreground compression. Therefore, we are supposed to perform morphological processing such as thresholding, dilation and open operation on the original foreground mask m_t to get a cleaner mask. In practice, if we compress the background regions around foreground objects together when performing foreground compression, the transition between the foreground and background in the final decoded frame will be more harmonious. Therefore, we apply the simple bounding rectangle search [31] to get the desired regular foreground mask $\widehat{m}_t$.
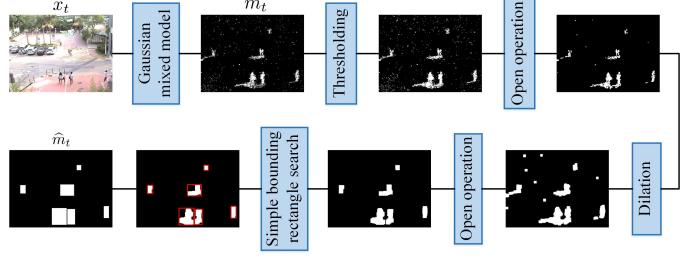

Fig. 3. Illustration of the adaptive Gaussian mixture model, morphological processing and simple bounding rectangle search.

D. Motion Compensation

The effect of motion compensation is essentially to obtain the predicted foreground $\widehat{f}_t$ based on the previous reconstruction foreground f_{t-1} and motion information $\widehat{v}_t$. Our method uses optical flow as motion information to achieve pixel-level motion compensation, which doesn't require complex operations such as loop filtering as in the conventional block-based method. The overall architecture of our proposed method is shown in Fig. 4.

First, we can get the wrapped foreground w_t with the following remapping formula:

$$f_{t-1}(x,y) = w_t(x + v_x, y + v_y) \quad (2)$$

where (x, y) is a point in f_{t-1} and (v_x, y_y) represents the motion information of point (x, y) from time $t-1$ to time t. Then we contact the f_{t-1}, w_t and v_t along the channel axis into a feature map and input it into the compensation network (Com-Net) to obtain the predicted foreground $\widehat{f}_t$. The specific structure of the Com-Net is provided in the appendix.
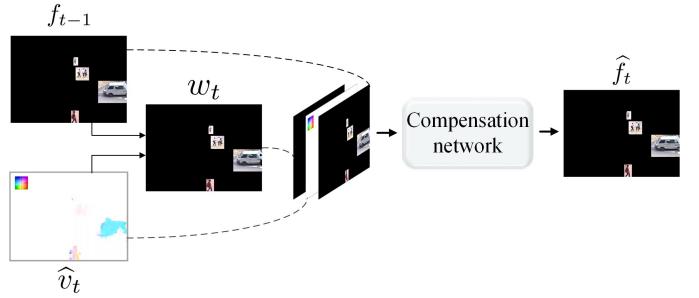

Fig. 4. Illustration of the motion compensation module.

E. Coarse-to-fine Two-stage Decoding Module

The function of the composite module is to combine the reconstructed foreground $\overline{f}_t$ with the reconstructed background $\widehat{b}_t$ to produce a composite frame $\widehat{x}_t$. As shown in Fig. 5, the specific method is to replace the corresponding position of the reconstructed background $\widehat{b}_t$ with the foreground $\overline{f}_t$ according to the foreground mask p_t ($\widehat{m}_t$ in autoencoder method). However, the foreground and background in the composite frame $\widehat{x}_t$ may not be well merged, and there may be transition boundaries and inconsistencies. We enhance the
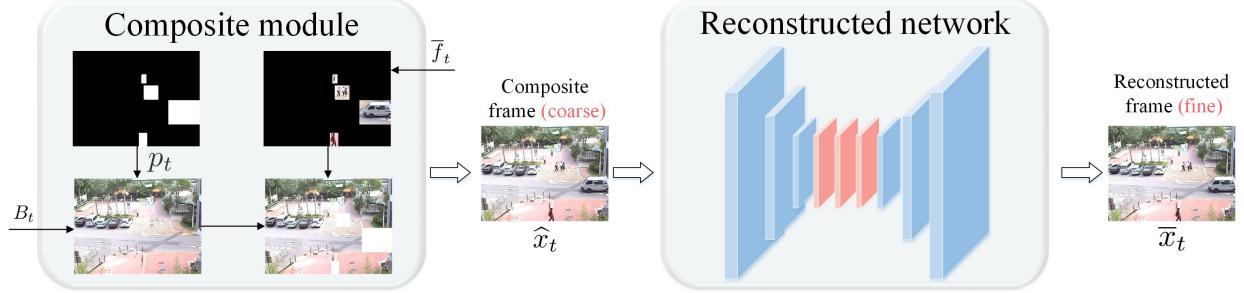
Fig. 5. Illustration of a coarse-to-fine, two-stage module, which is composed of a composite module and a reconstruction network (Rec-Net). The composite module embeds the reconstructed foreground $\overline{f}_t$ in the corresponding position of the reconstructed background $\widehat{b}_t$. The quality of the composite frame $\widehat{x}_t$ is enhanced by the Rec-Net to eliminate distortion such as artifacts, boundaries and blurs. The blue planes in Rec-Net represent the convolution and transposed convolutional layers, and the red planes represent the residual blocks.

quality of the composite frame $\widehat{x}_t$ through the Rec-Net to make the foreground and background composited harmoniously.

As shown in Fig. 5, the Rec-Net is composed of a stack of three convolutional layers, three residual blocks, and three transposed convolutional layers. The specific network structure is provided in the appendix.

IV. IMPLEMENTATION

A. Training Strategy

We learn the parameters of the model by piecewise training. First, we perform pre-training on some modules in the architecture. We take several clips from the original video, feed them into the GMM sequentially, and compare the current extracted background with the previous one. When the backgrounds from the two adjacent frames are almost the same and no longer change, the pre-training of the GMM is completed. Besides, the network for optical flow estimation is initialized with the pretrained weights obtained from [32].

Then we train the information codec and Com-Net for foreground compression. The purpose of the training is to minimize the following foreground loss:

$$L_f = E\left[d\left(f_t, \overline{f}_t\right)\right] \quad (3)$$

The above loss measures the distortion of the foreground f_t and the reconstructed foreground $\overline{f}_t$. Here we use the Mean Square Error (MSE) to implement, that is, $d = (f_t - \overline{f}_t)^2$.

Finally, we perform the end-to-end training of the entire model include Rec-Net. The purpose of the training is to minimize the following overall loss:

$$L_x = E\left[d\left(x_t, \overline{x}_t\right)\right] \quad (4)$$

The overall loss is similar to the foreground loss. The main difference is that the similarity between the original frame x_t and the reconstructed frame $\overline{x}_t$ is measured here.

B. Quantization

To increase the compression ratio, the motion information v_t and the residual r_t need to be encoded and quantized. The selection of quantization bit is very important, because appropriate quantization bit not only improves the compression

ratio, but also reduces the distortion. In order to increase the compression ratio, we set $C_L = \{0, 1, 2, ..., 2^L\text{-}1\}$. There are plenty of methods to quantize the input to a number in C_L. Here we use the nearest neighbor quantization method [33] to compute:

$$\widehat{q} = Q(\omega) = \arg\min_j |\omega - c_j| \quad (5)$$

where $c_j = j$, and $j \in C_L = \{0, 1, 2, ..., 2^L\text{-}1\}$.

C. Bitstream Storage

In our method, the compression bitstreams of the foreground and background are indexed to facilitate retrieval. Specifically, as shown in Fig. 6, the compression bitstreams of the background templates are stored along with the background index of their frame number. Also, the foreground index indicates the corresponding frame number of each foreground and the frame range of non-foreground segments.
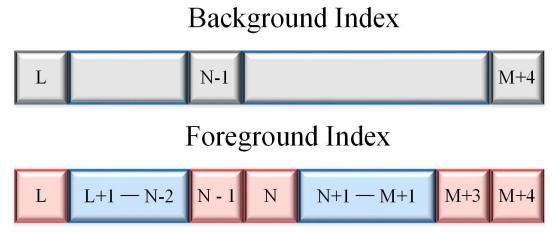

Fig. 6. Illustration of the background and foreground index.

V. EXPERIMENTS

A. Experiment Setup

1) Dataset: We train our model on surveillance video clips taken from CUHK Square Dataset [34] and EWAP Dataset [35]. The two datasets consist of three standard surveillance videos, which contain many different sizes of objects, such as cars, people and bicycles. What's more, there are changes in brightness with light and weather as in a natural environment. To remove artifacts induced by the previous compression, each of the above video frames is cropped and resized to $320 \times 240 \times 3$ before training. To compare with other video

compression algorithms, we test on the videos with the static background (Traffic, Cactus, BasketballDrill, Vidyo1, Vidyo3, Vidyo4) included in HEVC Dataset [3]. However, none of the above videos have a long duration (their duration is all 10 s), and they are also not standard surveillance scenarios. To demonstrate the superiority of our method specially designed for the low information density characteristics of surveillance videos, we take different clips from three surveillance videos in CUHK Square Dataset and EWAP Dataset for testing.

Finally, we contribute a novel idea that we can combine our compression algorithms with hardware design to perform adaptive sampling for the surveillance cameras. The sampling with a low sampling rate and low-resolution is performed when no foreground is detected in the current frame x_t. However, if the foreground objects appear in the current frame x_t, we will switch to a higher sampling rate and sample the foreground regions with high-resolution. We have verified our idea through software simulation and shown a few sample videos, which are put in the supplemental materials.

2) Evaluation Standard: The key to compression is to find a balance between the distortion and compression ratio, so the distortion and compression ratio are important basis for us to measure the performance of a compression algorithm. Here we use PSNR and MS-SSIM to measure the compression distortion. Besides, we use the average bits required to encode each pixel per frame (bpp) as a measure of the compression ratio. Finally, we will report the time it takes to compress and decompress each frame of the videos.

3) Parameter Settings: The quantization bit of the quantizer used in Step 5 of Sec. III-A is set to 1. In addition, the threshold parameter γ related to the background template updating frequency is set to 0.98. Besides, if not specially mentioned, the channel C in Step 5 of Sec. III-A is set to 8. Then we train the information codec and Com-Net with a learning rate of 2×10^{-4}. Finally, we perform the end-to-end training, and the learning rate is set to 2×10^{-5}.

B. Adaptive Background Template Updating Analysis

The background in the surveillance video has fluctuations, and there are subtle changes in the brightness and color of the background between two adjacent frames. The handcraft background template updating frequency often fails to respond to the changes in the natural environment in a timely manner, so we adopt an adaptive template updating algorithm. We select 900 frames from the test dataset and calculated the MS-SSIM value between the background extracted from each frame with the previous background template according to the background template updating algorithm as described in Sec. III-B. When the MS-SSIM value is smaller than 0.98, it indicates that the background has changed a lot, possibly because the sun is blocked by the cloud or at dusk.

As shown in Fig. 7, when the weather turns cloudy, the MS-SSIM value is smaller than 0.98, which is the moment when we need to update the background template. We can change the updating frequency of the background template by setting different threshold γ, thus changing the compression ratio.
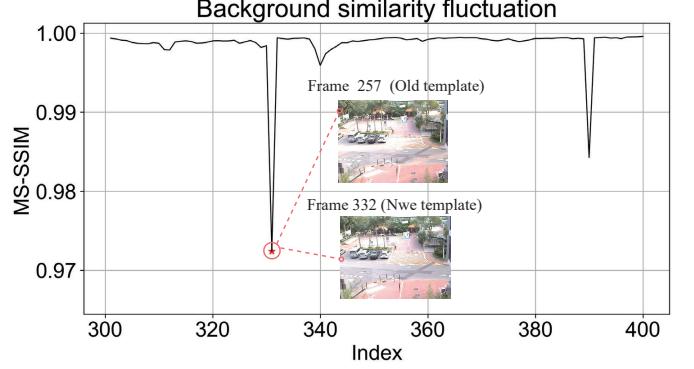

Fig. 7. Illustration of background fluctuations (Frame 300-400). The moment circled is when the background changes a lot and we need to update template.

C. Comparison Results

We compare our method with some conventional algorithms such as H.264, H.265 and the method BCBR [8] specially designed for surveillance video compression. We follow the settings in [5] to get frames compressed by the H.264 and H.265. In addition, the first and the latest end-to-end deep compression method KFI [6] and DVC [5] are also included in the comparison. Besides, we compare our method with the post-processing algorithm MFQE [18] which is used to optimize the performance of H.265. We use the above algorithms to obtain a set of PSNR values under different bpp, and average them over the test videos from the HECV dataset to produce the average PSNR. Finally, we draw the curves to characterize the performances of different compression methods.

As shown in Fig. 8, when evaluated by PSNR, our method outperforms other methods. The performance of KFI is close and slightly better than H.264, but much worse than H.265. The performance of DVC is slightly worse and slightly better than H.265 at low bpp and high bpp, respectively. Although BCBR is somewhat better than H.265 overall and MFQE improves the performance of H.265 by 0.5-1 dB, but there is still a big gap between their performance and ours. For example, to achieve the same PSNR (36 dB), our method requires 69.5% less bpp than H.265. As shown in Fig. 8, the two DNN-based
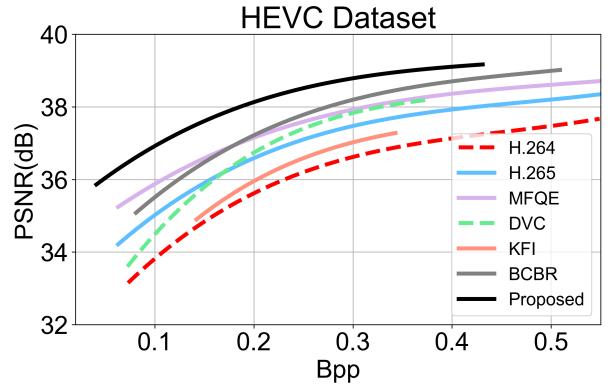

Fig. 8. Illustration of the comparison of our method with other conventional and DNN-based video compression methods.
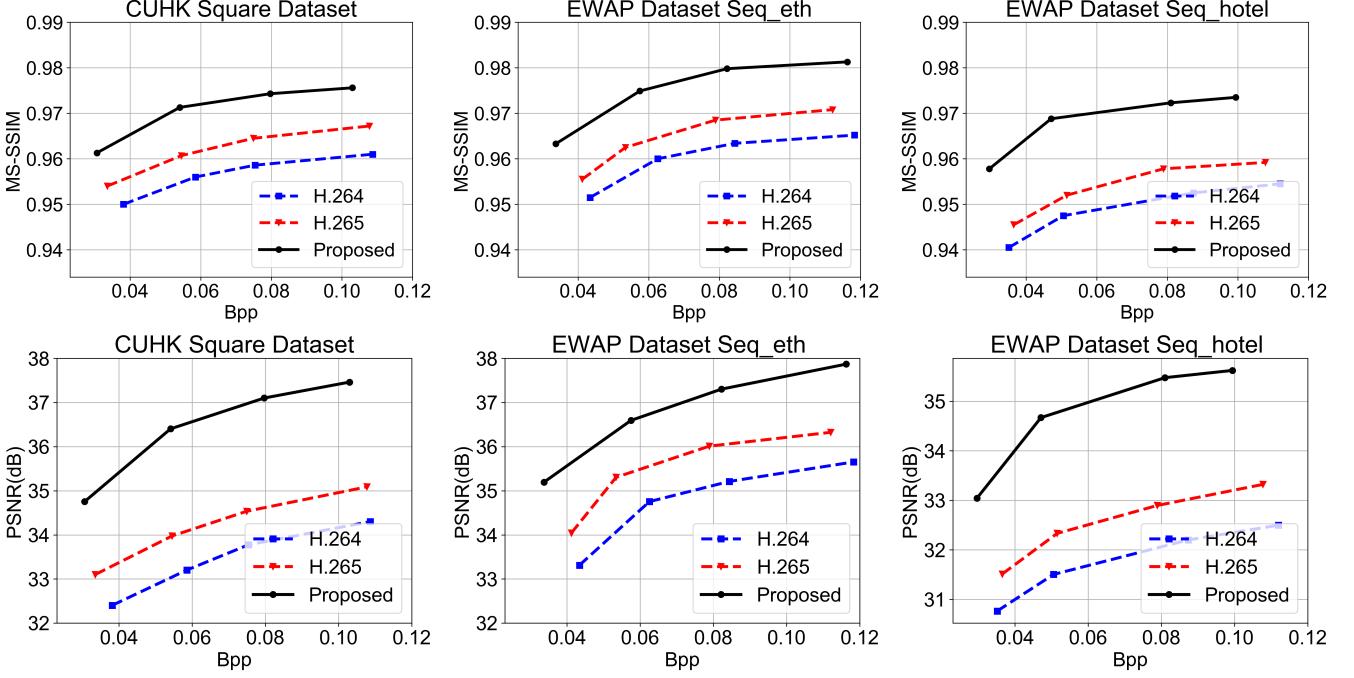
Fig. 9. Illustration of the comparison results on the CUHK Square Dataset and EWAP Dataset.

end-to-end methods are not as good in performance as the conventional method BCBR, because they're not specifically designed for surveillance video compression. Besides, we can see that our method has a greater advantage than other methods at low *bpp*. As *bpp* rises, the background compression algorithm gradually becomes an important factor for limiting performance improvement. Fortunately, the background compression algorithm is replaceable in our method. With the advent of algorithms with better performance, the performance of our method at high *bpp* can be further improved.

In addition to the above comparisons, we also test on the CUHK Square Dataset and EWAP Dataset and compare them with the compression results of H.264 and H.265. The comparison results are shown in Fig. 9. The compression performance of our method is much better than H.264 and H.265 in both MS-SSIM and PSNR. For example, our proposed method needs 70.01% and 45.9% less *bpp* (bits per pixel) to achieve the same MS-SSIM (0.96) than the conventional algorithms H.264 and H.265 on the CUHK Square Dataset, respectively.

D. Ablation Experiment

Based on the fluctuations of the video background, we replace the handcraft equal-interval updating with an Adaptive Background Template Updating (ABTU). In addition, unlike the one-step frame decoding method, we are inspired by [36] to enhance the frame quality through the Rec-Net.

Furthermore, to demonstrate the importance of temporal information for video compression, we compress the foreground through an autoencoder that directly encodes and decodes the foreground instead of the motion-based method described above. As shown in Fig .10, that is achieved by replacing Step 4-7 in Sec. III-A with the following three steps: (1) Under
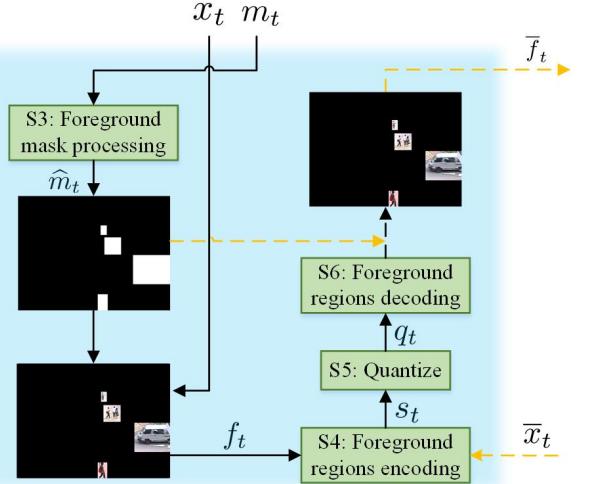

Fig. 10. Illustration of an autoencoder scheme that encodes and decodes the foreground directly.

the guidance of the mask $\widehat{m}_t$, we get the foreground f_t from the original frame x_t. Then we encode the f_t as bitstreams s_t directly. (2) The bitstreams s_t are quantized as q_t. (3) We decode q_t and reconstruct the foreground $\overline{f}_t$ under the guidance of $\widehat{m}_t$ directly. The specific foreground encoder and decoder are provided in the appendix.

To demonstrate the importance of the above three components, we have designed the following four models: (1) complete model (2) the model without Rec-Net (3) the model without ABTU (update every 50 frames). (4) the model with autoencoder. We train the above four models respectively, test on the CUHK Square dataset and then draw the results in the
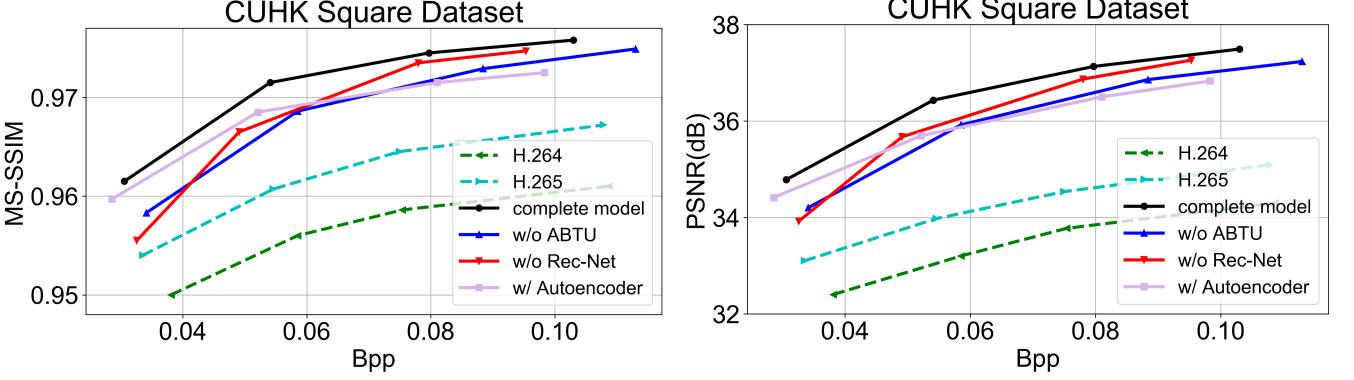
Fig. 11. Illustration of the results of the ablation experiment measured by MS-SSIM and PSNR. ABTU represents adaptive background template updating. Experimental results measured by PSNR can be found in supplemental materials.

same chart. As shown in Fig. 11, the lack of Rec-Net and adaptive template updating module damages performance to some extent. What's more, we find that the damage caused by removing the adaptive template updating is pronounced. This may be because the information density of the surveillance video is very low and the fixed handcrafted updating frequency we set is too high, which reduces the compression ratio required to maintain the same compression quality. Furthermore, although the performance of the autoencoder method is close to the motion-based method at low bpp, the gap between their performance widens as bpp increases. The main reason for it is that the autoencoder method does not make full use of the temporal information of the foreground.

E. Compression Stability Analysis

The proposed compression algorithm is expected to have strong stability, that is, the compression effects of different frames are similar, without large fluctuations. To test the stability of our method, we select a 300-frame video from the CUHK Square test set and compare the compression results of the background $\widehat{b}_t$, foreground $\widehat{f}_t$ and reconstructed frame $\widehat{x}_t$ with original ones. The background is obtained by linear interpolation described in Eq .1 and the CNN-based interpolation method proposed in [6], respectively. As shown in Fig .12, the background and the reconstructed frame have only small fluctuations, while the foreground has relatively large fluctuations due to the drastic changes that happened in the foreground regions. In addition, we surprisingly found that using the simplest linear interpolation and complex CNN interpolation, the stability of the two is very similar, mainly because the following two points: (1) The surveillance video usually has a static background, and the backgrounds at different times are highly similar; (2) The limiting factor of background stability is mainly residual coding, and the interpolation method is necessary but not decisive. Therefore, the linear interpolation is applied by default in the paper. As the statistical histogram of the MS-SSIM values shows in Fig .13, it can be seen that the compression of our method only fluctuates within a certain range. Besides, the histograms of the background and reconstructed frame are pyramidal, which shows relatively strong stability.
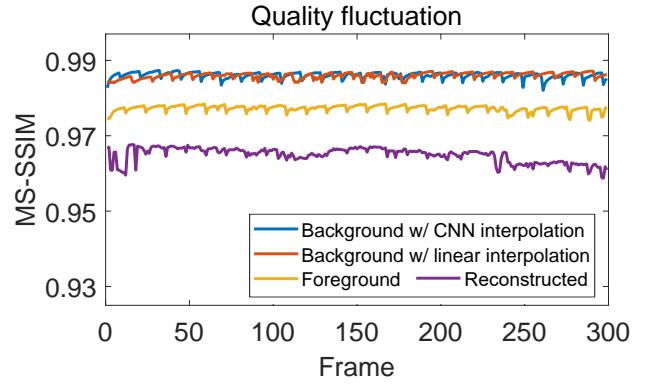

Fig. 12. Illustration of the compression quality fluctuation of the background $\widehat{b}_t$, foreground $\widehat{f}_t$ and reconstructed frame $\widehat{x}_t$ within a range of frames.
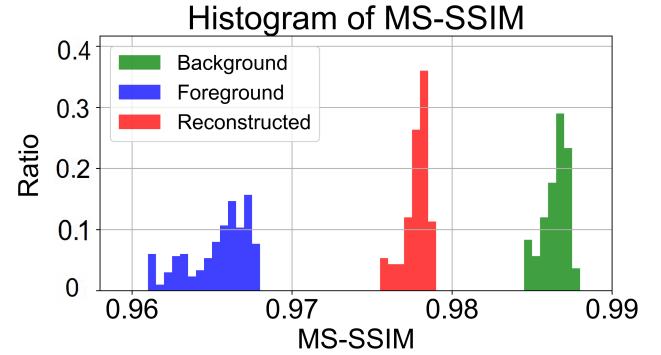

Fig. 13. Illustration of the statistical histogram of MS-SSIM values of the background $\widehat{b}_t$, foreground $\widehat{f}_t$ and reconstructed frame $\widehat{x}_t$. Note that the background is implemented with linear interpolation.

F. Analysis of the Proportion of Foreground

To analyze the impact of the proportion of the foreground on the compression performance, we analyze the relationship between the foreground ratio with bpp and MS-SSIM under different C (See Step 5 in Sec. III-A). As shown in Fig. 15, we find that bpp is approximately linear with the foreground ratio. In addition, as the foreground ratio increases, the compression
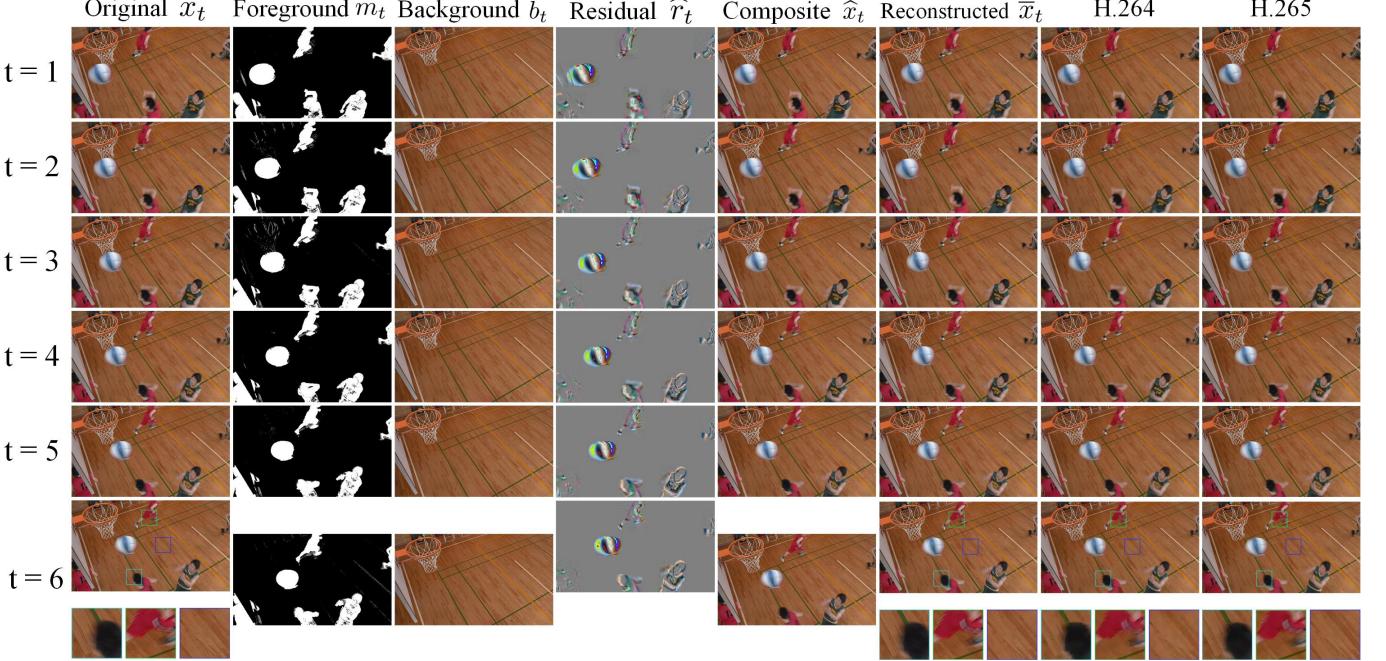
Fig. 14. Illustration of the intermediate results and the compression results of other algorithms. We zoom in on the local details of Frame 6, from which we can see that our compression results are visually better.
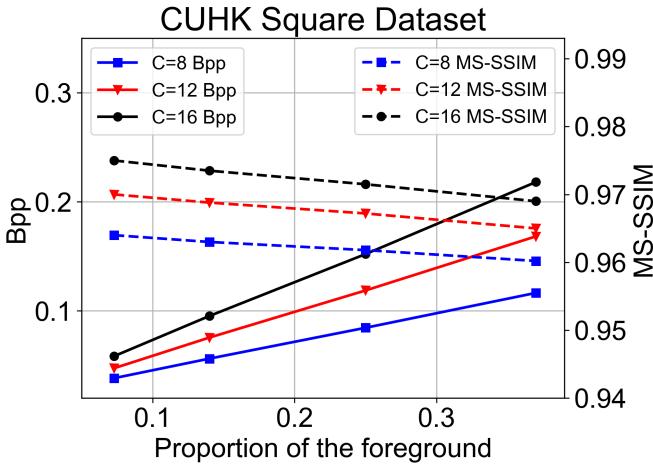

Fig. 15. Illustration of the relationship between the proportion of foreground and the compression performance.

quality gradually deteriorates, and the higher the foreground ratio, the worse the deterioration. This is because higher foreground ratio means that more contents in $\overline{x_t}$ come from reconstruction, which degrades the quality of the frame.

In the experiment, we consider the extreme situation when the pedestrian volume is very large so that the foreground ratio can reach nearly 40%. However, there are a large number of unmanned scenes in the real surveillance video and the foreground ratio is constantly fluctuating, so the average foreground ratio is often smaller than 15% in general. Therefore, bpp is generally less than 0.1, while MS-SSIM is generally higher than 0.96. In addition, we consider the other extreme

case when people and vehicles occasionally appear in the video, and the foreground ratio is less than 1%. At this time, the bpp may be less than 0.01, and the bits are mainly used for background compression.

G. Visual Comparison

As shown in Fig. 14, we present the intermediate results of compression, including the original frame x_t, foreground mask m_t, reconstructed background $\widehat{b}_t$, residual $\widehat{r}_t$, composite frame $\widehat{x_t}$, and reconstructed frame $\overline{x_t}$. Comparing $\widehat{b}_t$ with the original frame, we find that the Gaussian mixture model extracts the background well. Visually, the background $\widehat{b}_t$ is almost identical to the background in the original frame, without severe distortions such as artifacts, blurs, and boundaries.

In the composite frame $\widehat{x_t}$, the composition of the foreground and background template is not very harmonious due to the obvious boundaries. However, in the reconstructed frame optimized by the Res-Net, the boundaries are completely eliminated, and the transition between the foreground and the background is very consistent.

Finally, we give a comparison of our compression results with the commonly used conventional H.264 and H.265. In terms of surveillance video, since these conventional methods are not specifically designed based on the low information density characteristic of surveillance video, their results are not as pleasing as ours visually. In our method, some details of the video, such as the athlete's hair, the outline of the sports pants and the holes in the floor are well preserved.

H. Adaptive Sampling

1) Idea Introduction: We can combine our method with hardware design to allow the surveillance camera to adaptively
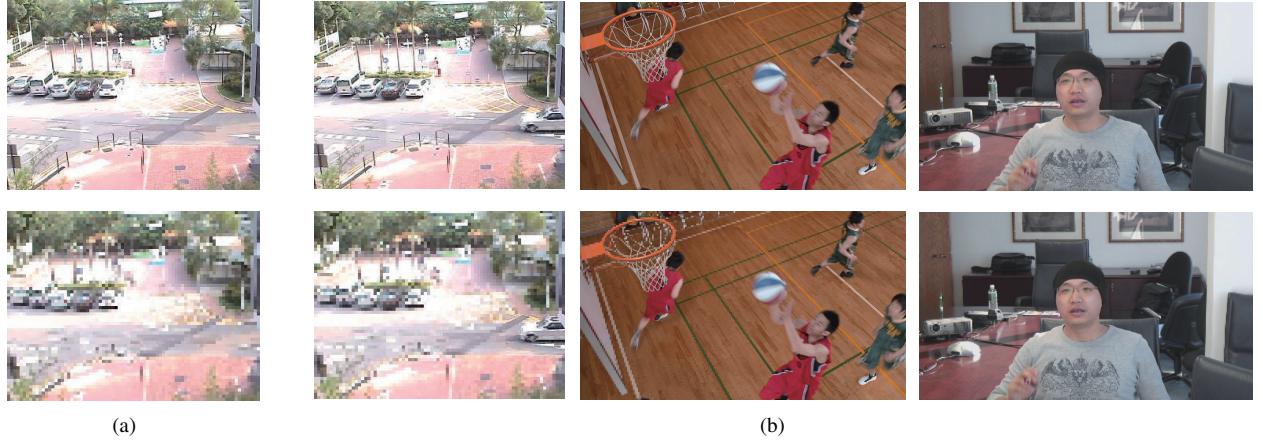
| (a) | (b) |

Fig. 16. Illustration of visual simulation results of adaptive sampling. Top: Original frames, bottom: adaptive sampling frames.

set the sampling rate and sampling resolution. The sampling with a low sampling rate and low resolution is performed when no foreground object is detected in the current frame. However, when the foreground objects appear in the current frame, we will switch to a higher sampling rate and sample resolution.

2) Software Simulation: We validate our ideas through software simulation. The specific implementation method is as follows. For a video, we can determine whether there are foreground objects based on the processed foreground mask $\widehat{m}_t$. If there is only background in the frame, the sampling rate and sampling resolution will be reduced to 1/4 of the original. If there are foreground objects in the frame, we will sample with original rate and resolution, and then combine the high-resolution foreground with the low-resolution background under the guidance of the processed foreground mask $\widehat{m}_t$.

3) Sample Videos: Based on the simulation results, we have created some sample videos. As shown in Fig. 16(a), when there is no foreground object, the sampling resolution is set to low, which helps to save compressed bits. However, if foreground objects appear in the frame as shown in Fig. 16(b), the foreground regions, such as cars, basketball, and figures, are high-resolution but the background regions are low-resolution.

VI. DISCUSSION

Conventional video compression algorithms have been widely developed and applied in recent decades. In recent years, many DNN-based compression algorithms have been proposed, but their architecture is basically the same as the conventional architecture, except that the components in the conventional architecture are now replaced with DNNs. The approach we propose in this paper is different from the conventional architectures, which is mainly designed for surveillance video compression.

We firmly believe that our proposed method can inspire researchers to propose new algorithms with wider application fields and superior compression performance. In a word, it seems promising to combine high-level vision, such as semantic segmentation, object classification and object detection with image/video compression.

VII. CONCLUSION

In this paper, we have proposed a new video compression method that uses the Gaussian mixture model to extract the foreground and background of videos separately. Besides, we have found the fluctuations of background and creatively designed an adaptive background updating and interpolation algorithm to adapt it to real-world scene changes. Moreover, we propose a motion-based method with residual encoding to compress the foreground. Finally, the coarse-to-fine two-stage module has been adopted to achieve the composition of the background and foreground and the enhancements of composite frames. Experimental results show that our method outperforms other algorithms visually and in terms of objective metric MS-SSIM and PSNR. Incorporating high-level vision, such as semantic segmentation, object classification and object detection into image/video compression may be a new and promising exploration direction.

APPENDIX A
NETWORK STRUCTURE

There are four convolutional neural networks that need to be introduced in detail in the appendix. They are information encoder and decoder, foreground encoder and decoder, compensation network (Com-Net) and reconstruction network (Rec-Net). The specific network structures are as follows. It is noted that "conv c64-k3-s2↓" represents a convolution layer with 64 filters of size 3×3 and a stride of 2. In the same way, "residual" and "transposed_conv" represent residual block and transposed convolution, respectively.

A. Information Encoder and Decoder

To increase the compression ratio, the information encoder and decoder mentioned in Step 5 of the Sec. III-A are applied to encode and decode the motion information v_t and the residual information r_t, respectively. The specific network structure is shown in Fig. 17.
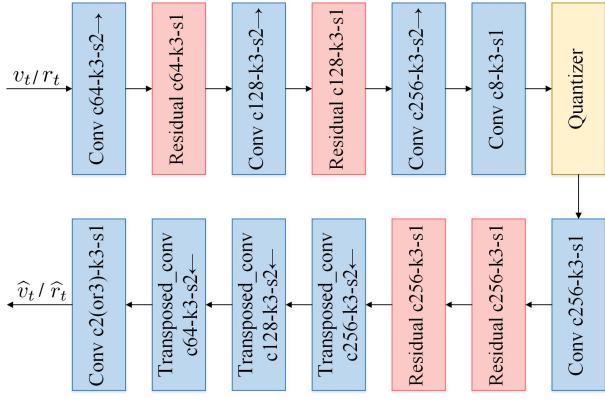
Fig. 17. Illustration of the information encoder and decoder.

B. Foreground Encoder and Decoder

We use the foreground encoder and decoder mentioned in Step 4-6 of Sec. V-D for encoding and decoding the foreground f_t directly. As is shown in Fig. 18, a fully convolutional neural network is used as the encoder, which consists of a crossover stack of several convolutional layers and residual blocks. Furthermore, we adopt the pyramidal decomposition scheme to our encoder. Let f_m denotes the input of the scale m layer, so f_1 denotes the original foreground f_t. $E_m(f_m)$ represents the output of the scale m. Then we set m to 1, 2 and 3 sequentially and execute encoding individually for each scale. The results of each scale are weighted and summed to produce an output $E(f_t) = E_1(f_1) + \frac{1}{2}E_2(f_2) + \frac{1}{4}E_3(f_3)$. Finally, $E(f_t)$ is convoluted with two convolutional layers to get the output s_t.

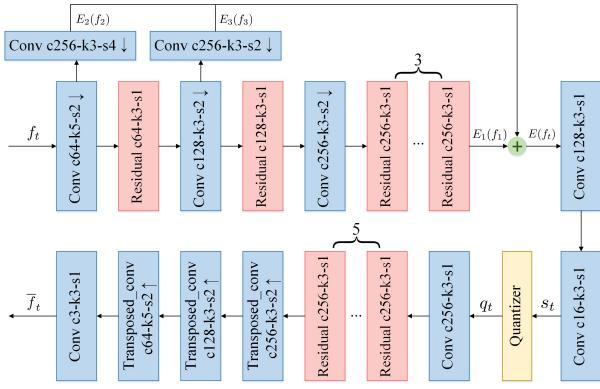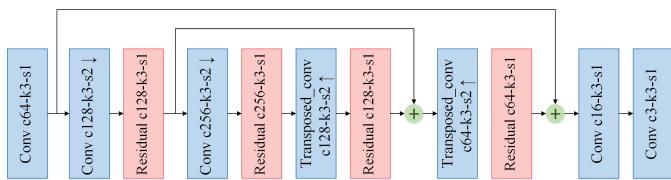Fig. 18. Illustration of the foreground encoder and decoder.

Fig. 19. Illustration of the compensation network.

C. Compensation Network (Com-Net)

The compensation network used for motion compensation is shown in Fig. 19. It inputs the concatenation of the wrapped foreground w_t, the previous reconstruction foreground $\overline{f}_{t-1}$ and motion information $\widehat{v}_t$ to obtain the predicted foreground $\widehat{f}_t$.

D. Reconstruction Network (Rec-Net)

The purpose of Rec-Net is to enhance the quality of the composite frame $\widehat{x}_t$ by eliminating block boundaries, blurring and other distortions, resulting in a better visual experience. The specific structure of Rec-Net is shown in Fig. 20.
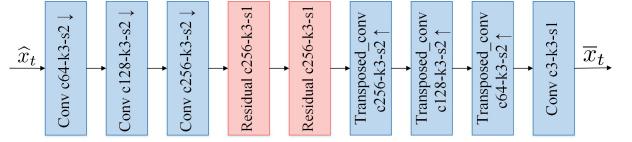

Fig. 20. Illustration of the reconstruction network (Rec-Net).

REFERENCES

[1] C. V. Networking Index, "Forecast and methodology, 2016-2021, white paper," *San Jose, CA, USA*, vol. 1, p. 1, 2016.

[2] T. Wiegand, G. J. Sullivan, G. Bjontegaard, and A. Luthra, "Overview of the h. 264/avc video coding standard," *IEEE Transactions on circuits and systems for video technology*, vol. 13, no. 7, pp. 560–576, 2003.

[3] G. J. Sullivan, J.-R. Ohm, W.-J. Han, and T. Wiegand, "Overview of the high efficiency video coding (hevc) standard," *IEEE Transactions on circuits and systems for video technology*, vol. 22, no. 12, pp. 1649–1668, 2012.

[4] S. Kim, J. S. Park, C. G. Bampis, J. Lee, M. K. Markey, A. G. Dimakis, and A. C. Bovik, "Adversarial video compression guided by soft edge detection," *arXiv preprint arXiv:1811.10673*, 2018.

[5] G. Lu, W. Ouyang, D. Xu, X. Zhang, C. Cai, and Z. Gao, "Dvc: An end-to-end deep video compression framework," in *Proceedings of the IEEE Conference on Computer Vision and Pattern Recognition*, 2019, pp. 11 006–11 015.

[6] C.-Y. Wu, N. Singhal, and P. Krahenbuhl, "Video compression through image interpolation," in *Proceedings of the European Conference on Computer Vision (ECCV)*, 2018, pp. 416–431.

[7] Z. Wang, E. P. Simoncelli, and A. C. Bovik, "Multiscale structural similarity for image quality assessment," in *The Thrity-Seventh Asilomar Conference on Signals, Systems & Computers, 2003*, vol. 2. Ieee, 2003, pp. 1398–1402.

[8] X. Zhang, T. Huang, Y. Tian, and W. Gao, "Background-modeling-based adaptive prediction for surveillance video coding," *IEEE Transactions on Image Processing*, vol. 23, no. 2, pp. 769–784, 2013.

[9] X. Zhang, L. Liang, Q. Huang, Y. Liu, T. Huang, and W. Gao, "An efficient coding scheme for surveillance videos captured by stationary cameras," in *Visual Communications and Image Processing 2010*, vol. 7744. International Society for Optics and Photonics, 2010, p. 77442A.

[10] F. Chen, H. Li, L. Li, D. Liu, and F. Wu, "Block-composed background reference for high efficiency video coding," *IEEE Transactions on Circuits and Systems for Video Technology*, vol. 27, no. 12, pp. 2639–2651, 2016.

[11] G. Wang, B. Li, Y. Zhang, and J. Yang, "Background modeling and referencing for moving cameras-captured surveillance video coding in hevc," *IEEE Transactions on Multimedia*, vol. 20, no. 11, pp. 2921–2934, 2018.

[12] C. Ma, D. Liu, X. Peng, L. Li, and F. Wu, "Traffic surveillance video coding with libraries of vehicles and background," *Journal of Visual Communication and Image Representation*, vol. 60, pp. 426–440, 2019.

[13] O. Rippel, S. Nair, C. Lew, S. Branson, A. G. Anderson, and L. Bourdev, "Learned video compression," *arXiv preprint arXiv:1811.06981*, 2018.

[14] I. Goodfellow, J. Pouget-Abadie, M. Mirza, B. Xu, D. Warde-Farley, S. Ozair, A. Courville, and Y. Bengio, "Generative adversarial nets," in *Advances in neural information processing systems*, 2014, pp. 2672–2680.

[15] S. Santurkar, D. Budden, and N. Shavit, "Generative compression," in *2018 Picture Coding Symposium (PCS)*. IEEE, 2018, pp. 258–262.

[16] A. X. Lee, R. Zhang, F. Ebert, P. Abbeel, C. Finn, and S. Levine, "Stochastic adversarial video prediction," *arXiv preprint arXiv:1804.01523*, 2018.

[17] E. Agustsson, M. Tschannen, F. Mentzer, R. Timofte, and L. Van Gool, "Generative adversarial networks for extreme learned image compression," *arXiv preprint arXiv:1804.02958*, 2018.

[18] R. Yang, M. Xu, Z. Wang, and T. Li, "Multi-frame quality enhancement for compressed video," in *Proceedings of the IEEE Conference on Computer Vision and Pattern Recognition*, 2018, pp. 6664–6673.

[19] Y. Hu, W. Yang, M. Li, and J. Liu, "Progressive spatial recurrent neural network for intra prediction," *IEEE Transactions on Multimedia*, 2019.

[20] J. Li, B. Li, J. Xu, and R. Xiong, "Intra prediction using fully connected network for video coding," in *2017 IEEE International Conference on Image Processing (ICIP)*. IEEE, 2017, pp. 1–5.

[21] S. Huo, D. Liu, F. Wu, and H. Li, "Convolutional neural network-based motion compensation refinement for video coding," in *2018 IEEE International Symposium on Circuits and Systems (ISCAS)*. IEEE, 2018, pp. 1–4.

[22] R. Yang, M. Xu, T. Liu, Z. Wang, and Z. Guan, "Enhancing quality for hevc compressed videos," *IEEE Transactions on Circuits and Systems for Video Technology*, 2018.

[23] Z. Liu, X. Yu, Y. Gao, S. Chen, X. Ji, and D. Wang, "Cu partition mode decision for hevc hardwired intra encoder using convolution neural network," *IEEE Transactions on Image Processing*, vol. 25, no. 11, pp. 5088–5103, 2016.

[24] A. Elgammal, D. Harwood, and L. Davis, "Non-parametric model for background subtraction," in *European conference on computer vision*. Springer, 2000, pp. 751–767.

[25] T. Liu, A. W. Moore, and A. G. Gray, "Efficient exact k-nn and nonparametric classification in high dimensions." in *NIPS*, 2003, pp. 265–272.

[26] A. Elgammal, R. Duraiswami, and L. S. Davis, "Efficient kernel density estimation using the fast gauss transform with applications to color modeling and tracking," *IEEE Transactions on Pattern Analysis & Machine Intelligence*, no. 11, pp. 1499–1504, 2003.

[27] C. Stauffer and W. E. L. Grimson, "Adaptive background mixture models for real-time tracking," in *Proceedings. 1999 IEEE Computer Society Conference on Computer Vision and Pattern Recognition (Cat. No PR00149)*, vol. 2. IEEE, 1999, pp. 246–252.

[28] N. Friedman and S. Russell, "Image segmentation in video sequences: A probabilistic approach," in *Proceedings of the Thirteenth conference on Uncertainty in artificial intelligence*. Morgan Kaufmann Publishers Inc., 1997, pp. 175–181.

[29] B. Klare and S. Sarkar, "Background subtraction in varying illuminations using an ensemble based on an enlarged feature set," in *2009 IEEE Computer Society Conference on Computer Vision and Pattern Recognition Workshops*. IEEE, 2009, pp. 66–73.

[30] P. KaewTraKulPong and R. Bowden, "An improved adaptive background mixture model for real-time tracking with shadow detection," in *Video-based surveillance systems*. Springer, 2002, pp. 135–144.

[31] P.-f. Cheng, H.-w. Yan, and Z.-h. Han, "An algorithm for computing the minimum area bounding rectangle of an arbitrary polygon," *Journal of Engineering Graphics*, vol. 1, no. 1, pp. 122–126, 2008.

[32] E. Ilg, N. Mayer, T. Saikia, M. Keuper, A. Dosovitskiy, and T. Brox, "Flownet 2.0: Evolution of optical flow estimation with deep networks," in *Proceedings of the IEEE conference on computer vision and pattern recognition*, 2017, pp. 2462–2470.

[33] L. Theis, W. Shi, A. Cunningham, and F. Huszár, "Lossy image compression with compressive autoencoders," *arXiv preprint arXiv:1703.00395*, 2017.

[34] M. Wang, W. Li, and X. Wang, "Transferring a generic pedestrian detector towards specific scenes," in *2012 IEEE Conference on Computer Vision and Pattern Recognition*. IEEE, 2012, pp. 3274–3281.

[35] S. Pellegrini, A. Ess, K. Schindler, and L. Van Gool, "You'll never walk alone: Modeling social behavior for multi-target tracking," in *2009 IEEE 12th International Conference on Computer Vision*. IEEE, 2009, pp. 261–268.

[36] W. Xiong, W. Luo, L. Ma, W. Liu, and J. Luo, "Learning to generate time-lapse videos using multi-stage dynamic generative adversarial networks," in *Proceedings of the IEEE Conference on Computer Vision and Pattern Recognition*, 2018, pp. 2364–2373.

Lirong Wu is currently pursuing the B.S. degree with the the Department of Information Science & Electronic Engineering, Zhejiang University, Hangzhou, China. His current research interests include machine learning and image/video processing.

Kejie Huang (M13-SM18) received his Ph.D degree from the Department of Electrical Engineering, National University of Singapore (NUS), Singapore, in 2014. He has been a principal investigator at College of Information Science Electronic Engineering, Zhejiang University (ZJU) since 2016. Prior to joining ZJU, he spent five years in the industry including Samsung and Xilinx, two years in the Data Storage Institute, Agency for Science Technology and Research (A*STAR), and another three years in Singapore University of Technology and Design (SUTD), Singapore. He has authored or coauthored more than 30 scientific papers in international peer-reviewed journals and conference proceedings. He holds four granted international patents, and another eight pending ones. His research interests include architecture and circuit optimization for reconfigurable computing systems and neuromorphic systems, machine learning, and deep learning chip design. He is the Associate Editor of the IEEE TRANSACTIONS ON CIRCUITS AND SYSTEMS-PART II: EXPRESS BRIEFS.

Haibin Shen is currently a Professor with Zhejiang University, a member of the second level of 151 talents project of Zhejiang Province, and a member of the Key Team of Zhejiang Science and Technology Innovation. His research interests include learning algorithm, processor architecture, and modeling. His research achievement has been used by many major enterprises. He has published more than 100 papers on academic journals, and he has been granted more than 30 patents of invention. He was a recipient of the First Prize of Electronic Information Science and Technology Award from the Chinese Institute of Electronics, and has won a second prize at the provincial level.

Lianli Gao is currently a Professor in University of Electronic Science and Technology under the 'UESTC 100 Young Talent' Plan. She obtained her PhD degree in Information Technology from The University of Queensland, Brisbane, Australia. Her research interests mainly include Deep Learning, Computer Vision, Visual and Language Fusion. She has published 90+ peer-reviewed papers in peer-reviewed conferences and Journals, including TPAMI, IJCV, TIP, AAAI, CVPR, etc. She has been a Guest Editor of Journal of Visual Communication and Image Representation, and Session Chair of IJCAI'19.